CHEMISTRY
A EUROPEAN JOURNAL

DOI: 10.1002/chem.200501340

Construction of Open Metal–Organic Frameworks Based on Predesigned Carboxylate Isomers: From Achiral to Chiral Nets

Daofeng Sun,[a] David J. Collins,[a] Yanxiong Ke,[a] Jing-Lin Zuo,[b] and Hong-Cai Zhou*[a]

Abstract: The four-connected carboxylate ligand *N*,*N*,*N*′,*N*′-tetrakis(4-carboxyphenyl)-1,4-phenylenediamine (TCPPDA) exists as three stereoisomers: a pair of enantiomers ($^{\delta}D_2$- and $^{\lambda}D_2$-TCPPDA) and a diastereomer (C_{2h}-TCPPDA). TCPPDA was predesigned for the construction of isomeric coordination networks. Reactions of $M(NO_3)_2$ (M = Cu, Zn, Co) or $Nd(NO)_3$ with TCPPDA under solvothermal conditions gave rise to five novel porous metal–organic frameworks: $[Cu_2(D_2\text{-tcppda})(H_2O)_2]\cdot 2\,DMSO\cdot 6\,H_2O$ (**1**), $[Cu_2(C_{2h}\text{-tcppda})(H_2O)_2]\cdot 2\,DMSO\cdot 6\,H_2O$ (**2**), $[Co_3(D_2\text{-Htcppda})_2]\cdot 4\,DEF\cdot 5\,H_2O$ (**3**), $[Nd_2(D_2\text{-tcppda})(C_{2h}\text{-tcppda})_{0.5}(DMSO)_3]\cdot 3\,DMSO\cdot 5\,H_2O$ (**4**), and $[Zn_4O(D_2\text{-tcppda})_{1.5}]\cdot DMF\cdot H_2O$ (**5**) (DMSO = dimethyl sulfoxide, DEF = diethylformamide, DMF = dimethylformamide). Complexes **1** and **2** are supramolecular isomers, in which all the ligands adopt pseudotetrahedral (both $^{\delta}D_2$- and $^{\lambda}D_2$-TCPPDA) and rectangular (C_{2h}-TCPPDA) geometries, respectively. Both compounds connect paddlewheel secondary building units (SBUs) to form three-dimensional porous networks possessing PtS and NbO nets, respectively. In **3**, all ligands possess pseudotetrahedral (both $^{\delta}D_2$- and $^{\lambda}D_2$-TCPPDA) geometry and link hourglass SBUs to form a three-dimensional porous framework. Compound **4** contains all three stereoisomers (C_2-, $^{\delta}D_2$-, and $^{\lambda}D_2$-TCPPDA), thus, has both pseudotetrahedral and rectangular geometries. D_2-TCPPDA connects the binuclear neodymium units to generate a two-dimensional layer, further linked by C_{2h}-TCPPDA to create a three-dimensional open framework. In **5**, all the ligands possess pseudotetrahedral geometry (D_2-TCPPDA), as found in **1** and **3**. However, all the TCPPDA ligands in **5** appear as either the $^{\delta}D_2$ or the $^{\lambda}D_2$ form, thus, the whole structure is homochiral. Complex **5** crystallizes in the $I4_132$ space group and the octahedral SBU in **5** is connected by the enantiopure TCPPDA to generate a three-dimensional porous network possessing the corundum Al_2O_3 net. Complexes **1**, **2**, and **5** possess permanent porosity, and **4** and **5** exhibit strong luminescence at $\lambda_{max} = 423$ and 424 nm, respectively, upon excitation at 268.5 nm.

Keywords: carboxylate ligands · chiral networks · crystal engineering · organic–inorganic hybrid composites · supramolecular chemistry

Introduction

Crystal engineering provides a powerful tool for the construction of metal–organic frameworks (MOFs).[1,2] Various secondary building units and organic ligands have been specifically designed for the synthesis of MOFs with desirable characteristics (porosity, chirality, fluorescence, magnetic properties, etc.) and topologies (perovskite, rutile, $SrSi_2$, PtS, NbO, etc.).[3] The geometries of the organic ligand and the metal or metal-cluster secondary building unit (SBU) are two important factors that always influence the topology of the final structure. By predesigning and selecting the organic ligand and the SBU, it is possible to construct novel coordination networks possessing a desired topology based on the geometries of the ligand and the SBU. However, recent developments in supramolecular isomerism and the interpenetration of structures have introduced more elements of complexity to the construction of MOFs and coordination networks, and have illuminated the difficulty in accurately predicting final structures.[4,5]

Supramolecular isomerism often results from the existence of several different building units with little or no difference in formation energy. Supramolecular isomers in-

[a] Dr. D. Sun, D. J. Collins, Dr. Y. Ke, Prof. Dr. H.-C. Zhou
Department of Chemistry and Biochemistry
Miami University, Oxford, Ohio 45056 (USA)
Fax: (+1) 513-529-8091
E-mail: zhouh@muohio.edu

[b] Dr. J.-L. Zuo
Coordination Chemistry Institute
State Key Laboratory of Coordination Chemistry
Nanjing University, Nanjing 210093 (China)

clude structural isomers,[1,6] in which atom connectivities differ, and stereoisomers, in which atom connectivities are identical. The latter encompasses diastereomers and enantiomers.[7] The study of supramolecular stereoisomerism can lead potentially to the generation of chiral coordination polymers from achiral ligands; however, the body of literature in this field is still limited.[8]

Controlled synthesis of MOFs remains a significant challenge to chemists, because the final structure is influenced by numerous factors, including ligand geometry, solvent, and reaction temperature.[9] In general, even seemingly minor changes in any of these factors can result in the formation of a different structural topology. Most ligands used in the study of supramolecular isomerism are derivatives of pyrrole or pyridine,[5,10] however, we recently designed a new tetracarboxylate ligand, the tetra-anion of *N*,*N*,*N*′,*N*′-tetrakis(4-carboxyphenyl)-1,4-phenylenediamine (TCPPDA) (Figure 1), which was chosen intentionally to lead to potential supramolecular isomers. This ligand has three stereoisomers: a pair of enantiomers (D_2 symmetry) and a diastereomer (C_{2h} symmetry). Despite our early preliminary work with this ligand, which revealed temperature-dependent supramolecular stereoisomerism,[11] the potential of this ligand to form novel supramolecular structures remained largely unexplored; conceivable structures could contain both C_{2h} and D_2 isomers, or possibly only one type of D_2 isomer (δ or λ). Furthermore, the size, shape, and nonplanarity of TCPPDA may hinder the formation of interpenetrating networks, which makes it a good choice for the construction of these networks.

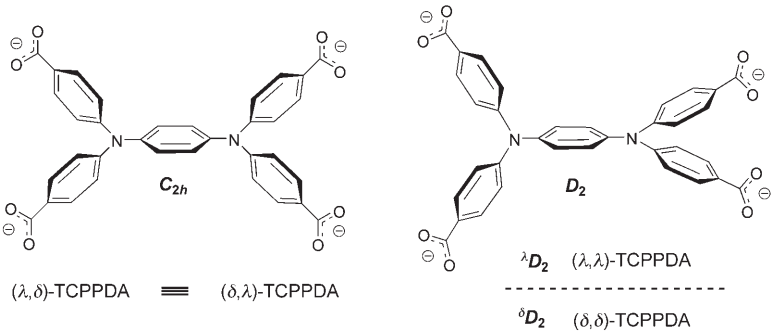

Figure 1. The designed tetracarboxylate ligand TCPPDA.

In the past decade, a large number of coordination networks or MOFs have been constructed from various organic ligands with different geometries and functionalities;[12] however, the designed construction of MOFs that exploits ligand isomerism is quite rare.[9] To extend our previous work, we have endeavored to carry out a systematic study of this ligand by employing different metal ions and clusters and by varying reaction conditions. Here, we describe the details of the syntheses, characterizations, and properties of MOFs based on this predesigned carboxylate ligand and its isomers.

Results and Discussion

The tetracarboxylate ligand TCPPDA was synthesized in two steps through an amination reaction and subsequent hydrolysis (Scheme 1). We selected TCPPDA as a target ligand in the study of supramolecular stereoisomerism and construction of MOFs primarily for the isomeric possibilities it presents. TCPPDA has three stereoisomers (a pair of enantiomers and a diastereomer); the diastereomer has C_{2h} symmetry with three phenyl rings oriented as left- and right-handed propellers around the two nitrogen atoms. A plane of symmetry exists through the central phenyl ring, reflecting one nitrogen-centered propeller with respect to the other. All four carboxylate carbon atoms lie within the same plane and define a rectangle; in a coordination network, the C_{2h} isomer will be a four-connected unit similar to a square-planar connector. The pair of enantiomers possess D_2 symmetry. In one case, both nitrogen-centered propellers are right-handed ($^{\delta}D_2$), and in the other case, both nitrogen-centered propellers are left-handed ($^{\lambda}D_2$). The conversion of the isomer from C_{2h} to D_2 will take place if the direction of one propeller is inverted by rotating two nitrogen–carboxyphenyl bonds on the same side of the central phenyl ring. The interconversion between the $^{\delta}D_2$ and $^{\lambda}D_2$ isomers can occur by inversion of both propellers, through rotation of all four nitrogen–carboxyphenyl bonds. The four carboxylate carbon atoms occupy the vertices of a stretched tetrahedron; in a coordination network, the D_2 enantiomers will be four-con-

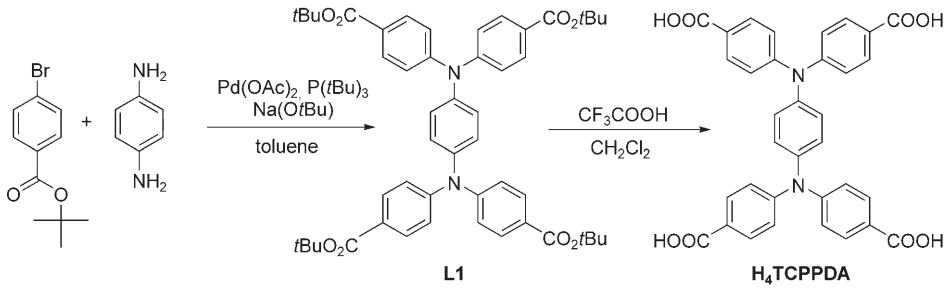

Scheme 1. The synthesis of H_4TCPPDA.

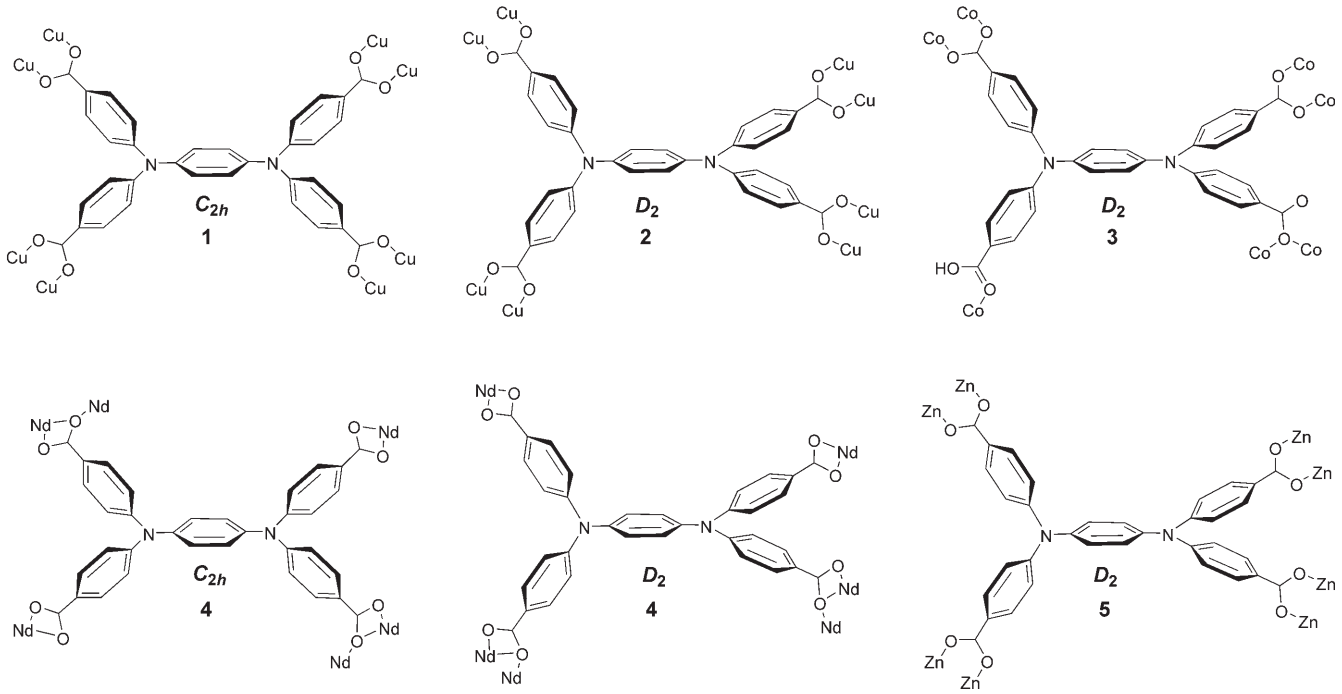

Figure 2. The coordination modes of TCPPDA in **1**–**5**.

nected units similar to tetrahedral connectors. The energy barrier for the inversion of a propeller should be low enough that TCPPDA can exist in all three forms in solution at room temperature. However, in a coordination network, it is possible that one of the three isomers will be favored over the others. If the pseudotetrahedral and rectangular geometries of the ligand can independently connect a rigid SBU, supramolecular isomers can be expected; furthermore, if D_2-TCPPDA appears in a structure as solely the ${}^{\delta}D_2$ or ${}^{\lambda}D_2$ form, a chiral MOF will result.

With these considerations in mind, we first attempted to incorporate this ligand into a coordination network with the copper(II) ion, due to its known propensity to form paddlewheel SBUs with carboxylate ligands. The solvothermal reaction of H_4TCPPDA and $Cu(NO_3)_2{\cdot}2.5\,H_2O$ in dimethylsulfoxide (DMSO) at 120 °C resulted in yellow crystals of **1**, $[Cu_2(D_2\text{-tcppda})(H_2O)_2]{\cdot}2\,DMSO{\cdot}6\,H_2O$, which possesses the PtS network in which all ligands adopt the pseudotetrahedral geometry (D_2-TCPPDA). However, the same reaction carried out at 115 °C results in burgundy-red crystals of **2**, $[Cu_2(C_{2h}\text{-tcppda})(H_2O)_2]{\cdot}2\,DMSO{\cdot}6\,H_2O$, which possesses the NbO network in which all ligands adopt rectangular geometry (C_{2h}-TCPPDA).[13] As indicated above, **1** and **2** were reported previously;[11] they will, therefore, be discussed further only in relation to the additional studies described herein.

Heating a mixture of H_4TCPPDA and $Co(NO_3)_2{\cdot}6\,H_2O$ in diethylformamidine (DEF) to 120 °C for four days resulted in the formation of red-violet crystals of **3**, $[Co_3(D_2\text{-}Htcppda)_2]{\cdot}4\,DEF{\cdot}5\,H_2O$. X-ray diffraction analysis revealed that **3** has a three-dimensional porous network containing a trinuclear cobalt cluster. One of the carboxylate groups of TCPPDA remains protonated, indicated by a C–O bond length of 1.283 Å, and by IR data, in which a strong absorption peak at around 1700 cm^{-1} for –COOH is observed. As shown in Figure 2, each TCPPDA molecule is seven-coordinate in the following manner: two carboxylate groups adopt bidentate bridging modes linking two cobalt atoms each; one carboxylate oxygen bridges two cobalt atoms; the protonated carboxylate group coordinates one cobalt atom in a monodentate coordination mode. Carboxylate groups from six different TCPPDA ligands connect three cobalt atoms arranged linearly to form a trinuclear "hourglass" SBU, as shown in Figure 3. Note that the central cobalt atom is octahedrally coordinated, whereas the two terminal cobalt atoms are tetrahedrally coordinated. This hourglass SBU is quite different from another hourglass SBU characterized previously in our laboratory, in which all the carboxylate groups adopt a bidentate bridging mode and two coordinat-

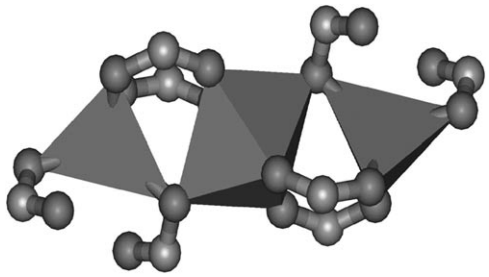

Figure 3. The hourglass SBU in **3**. Cobalt atoms are represented as polyhedra.

ed water molecules occupy the terminal positions.[14] The average Co–O distance is 2.037(6) Å. Each of the TCPPDA ligands in **3** has D_2 symmetry and is, therefore, chiral. However, because the ratio of ${}^{\delta}D_2$- to ${}^{\lambda}D_2$-TCPPDA in this network is 1:1, the coordination network is racemic overall.

The D_2-TCPPDA in **3** can be considered to be an elongated tetrahedral connector: the dihedral angle between the two planes, each defined by a nitrogen atom and the accompanying carboxylate carbon atoms, is 74.5°. Each TCPPDA ligand links four hourglass SBUs, and every SBU can be considered as an eight-connected node. Thus, the TCPPDA ligand connects hourglass SBUs to generate an eight-connected network structure with open channels (Figure 4). The

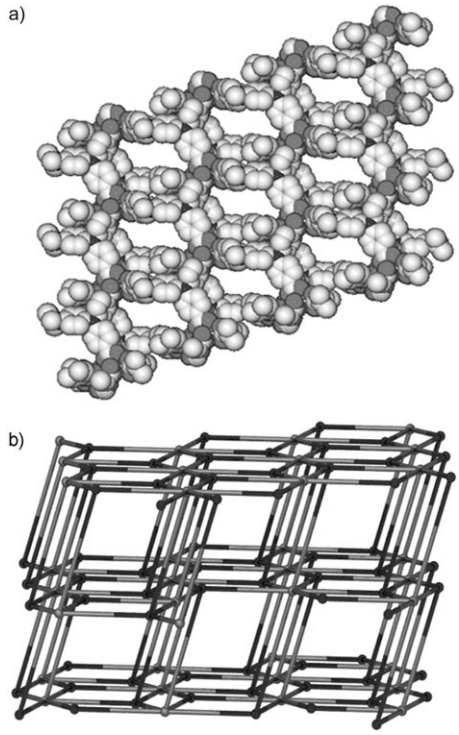

Figure 4. a) The three-dimensional porous framework of **3** viewed along the *b* axis. b) A schematic representation of **3** simplifying the organic ligand as a pseudotetrahedral connector and the hourglass SBU as an eight-connected node.

dimensions of the channels are 7.149×10.832 Å, in which free solvates reside. The structure is noninterpenetrated with a total potential solvent-accessible volume of 58% (1519.1 Å^3 per 2619.6 Å^3), as calculated by PLATON.[15]

In **1**, **2**, and **3**, all the TCPPDA ligands adopt only a single geometry, either pseudotetrahedral or rectangular. This is probably a result of the coordination geometry imposed by the first-row transition-metal ions, which typically adopt a low coordination number. The solvothermal reaction of H_4TCPPDA and $Nd(NO_3)_3{\cdot}6H_2O$ in DMSO at 120°C for 48 h resulted in light-yellow rodlike crystals of **4**, $[Nd_2(D_2\text{-tcppda})(C_{2h}\text{-tcppda})_{0.5}(DMSO)_3]{\cdot}3DMSO{\cdot}5H_2O$. X-ray diffraction analysis reveals that **4** also has a three-dimensional, noninterpenetrated porous framework. The lack of a strong IR absorption peak at 1700 cm^{-1} (for −COOH) indicates that all carboxylates are deprotonated during the reaction and formation of the network. Within the structure of **4**, there are 1.5 crystallographically independent ligands, and two different geometries of the ligand are present, C_{2h}- and D_2-TCPPDA. Both TCPPDA ligands have similar coordination modes: two carboxylate groups adopt a bidentate chelating mode, chelating one neodymium atom each, and the other two carboxylate groups adopt a chelating-bridging mode, connecting two neodymium atoms each, as shown in Figure 2. As in **3**, D_2-TCPPDA forms an elongated tetrahedral connector, with a dihedral angle between the two carboxylate-nitrogen-carboxylate planes of 63.6°. In contrast, all the carboxylate carbon atoms are coplanar in C_{2h}-TCPPDA. As in **3**, the coordination network is racemic overall, due to a 1:1 ratio of the ${}^{\delta}D_2$- to ${}^{\lambda}D_2$-TCPPDA enantiomers.

In **4**, two crystallographically independent neodymium atoms, Nd1 and Nd2, are connected by one TCPPDA ligand to form a binuclear Nd_2 unit. Both neodymium atoms adopt a nine-coordinate geometry: Nd1 is coordinated by two oxygen atoms from C_{2h}-TCPPDA, six from D_2-TCPPDA, and one from a coordinated DMSO molecule; Nd2 is coordinated by three oxygen atoms from C_{2h}-TCPPDA, four from D_2-TCPPDA, and two from coordinated DMSO. Each C_{2h}-TCPPDA connects four Nd2 atoms to generate a one-dimensional chain, in which the Nd2···Nd2 distance is 13.440 Å, as shown in Figure 5. Each D_2-TCPPDA links four

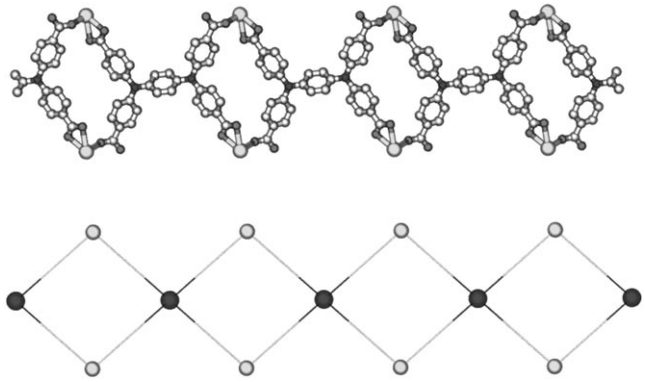

Figure 5. The one-dimensional chain in **4** connected by C_{2h}-TCPPDA.

Nd1 atoms to give rise to a two-dimensional layer framework, in which the Nd1···Nd1 distance is 13.109 Å (Figure 6). The one-dimensional chains and two-dimensional layers are further connected by the carboxylate groups of C_{2h}- or D_2-TCPPDA in a chelating or bridging mode to give rise to a three-dimensional, noninterpenetrated porous framework, as shown in Figure 7. The Nd1···Nd2 distance along the *a* axis is 3.850 Å. The dimensions of the channels are 10.558×19.316 Å, in which free solvates reside. The sol-

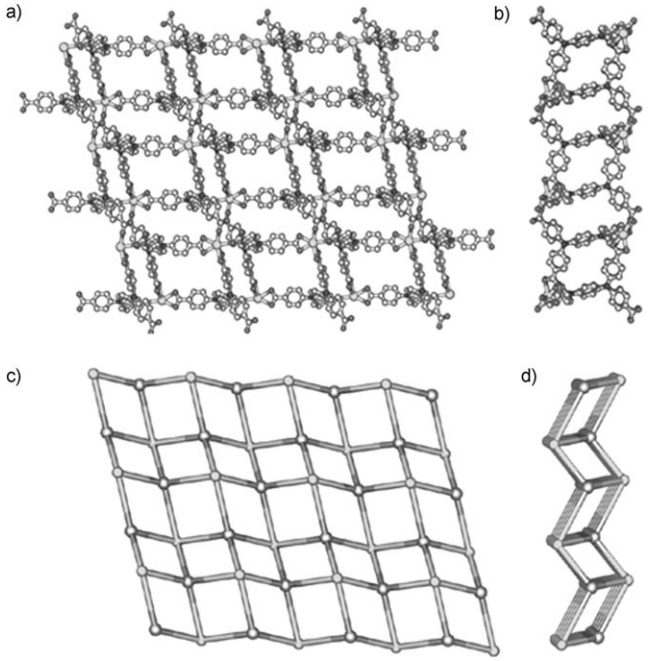

Figure 6. The two-dimensional layer in **4** connected by D_2-TCPPDA. a) Viewed along the *c* axis. b) Viewed along the *a* axis. c) and d) Schematic representations of the same views, simplifying the organic ligand as a pseudotetrahedral connector.

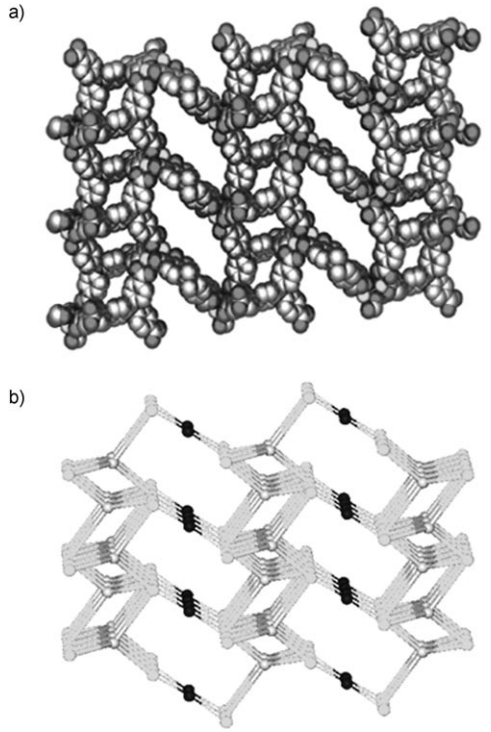

Figure 7. The three-dimensional porous framework of **4** viewed along he *a* axis. a) The three-dimensional porous framework of **4** viewed along the *a* axis. b) A schematic representation of **4**, simplifying the organic ligand as pseudotetrahedral and rectangular connectors.

vent-accessible volume is 67.9% (4059.0 Å^3 per 5977.3 Å^3), calculated by PLATON.[15]

1, **3**, and **4** all have a racemic network, due to the 1:1 ratio of $^{\delta}D_2$- to $^{\lambda}D_2$-TCPPDA within the network. However, if a synthesis results in all the D_2-TCPPDA ligands appearing as either the $^{\delta}D_2$ or the $^{\lambda}D_2$ form, then the overall network will be chiral rather than achiral. The solvothermal reaction of $Zn(NO_3)_2{\cdot}6H_2O$ and H_4TCPPDA in dimethylformamide (DMF) at 120 °C results in the formation of red block crystals of **5**, $[Zn_4O(D_2\text{-tcppda})_{1.5}]{\cdot}DMF{\cdot}H_2O$. Although the bulk sample of **5** is racemic, individual crystals self-assemble into separate chiral enantiomeric structures with ligands in the form of either all $^{\delta}D_2$ or all $^{\lambda}D_2$.

All the carboxylate groups of TCPPDA are deprotonated during the reaction, with each carboxylate connecting two zinc atoms in a bridging mode. Four zinc atoms are linked by six carboxylate groups from different TCPPDA ligands and one μ_4-oxygen atom to form a $Zn_4O(OOCR)_6$ unit, a basic carboxylate octahedral SBU (Figure 8a). Two crystallographically independent D_2-TCPPDA units appear in the structure; the carboxylate-nitrogen-carboxylate dihedral angles are 77.1 and 85°. Each TCPPDA ligand connects four octahedral SBUs (Figure 8b) and each octahedral SBU attaches to six TCPPDA ligands to give a three-dimensional porous framework with two kinds of channels (Figure 9). The dimensions of the channels are 7.007 × 7.007 Å (**A**) and 9.510 × 9.510 Å (**B**), in which DMF and water solvates reside. The structure is noninterpenetrating, due to the nonplanarity of the ligand and the rigidity of the SBU, and has a total solvent-accessible volume of 74.7% (42068.2 Å^3 per 56342.0 Å^3), as calculated by PLATON.[15]

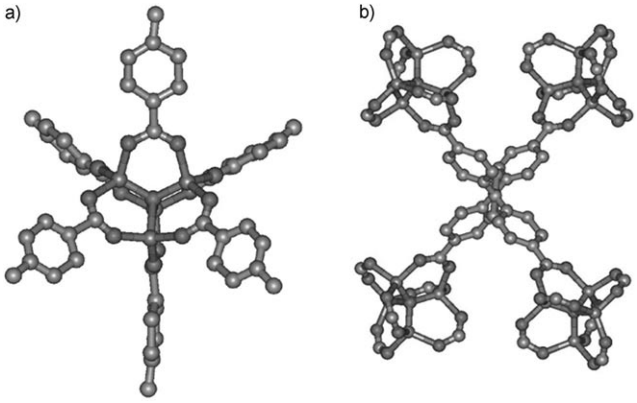

Figure 8. a) The basic carboxylate octahedral SBU, $Zn_4O(OOCR)_6$, in **5**. b) Each TCPPDA ligand connects four octahedral SBUs.

Although it is difficult to combine tetrahedral organic ligands and octahedral metal SBUs in the construction of MOFs, it has been shown that the best compromise between these two forms is found in the corundum form of Al_2O_3 (α-alumina), in which both aluminum and oxide ions are distorted from their ideal geometries.[16,17] To further understand the topology of **5** as an analogue of the corundum topology, simplified models of the ligand and the SBU cluster can be considered: as discussed above, the organic ligand

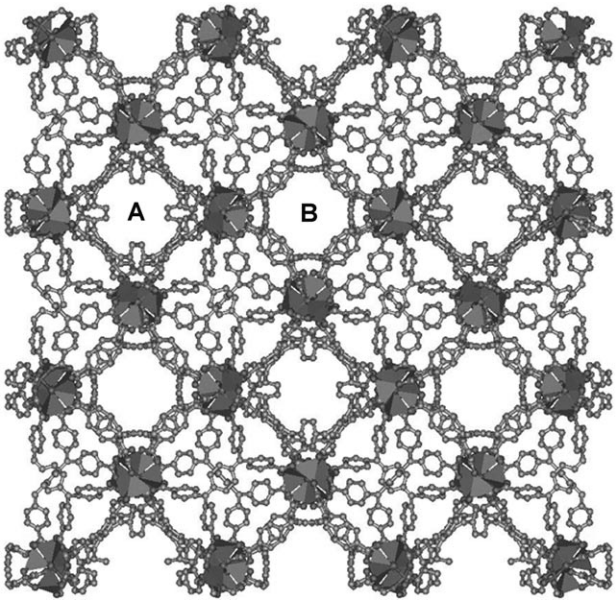

Figure 9. The three-dimensional porous framework of **5**. The two unique types of channels are labeled **A** and **B**. Zinc atoms are represented as tetrahedra.

can be modeled as a tetrahedral connector, and the SBU cluster can be modeled as an octahedral node with the μ_4-oxygen atom at the center. The resulting corundum topology is shown in Figure 10. Recently, Moorthy et al. reported zinc and cadmium coordination networks possessing the corundum topology constructed from a D_{2d}-symmetric pyridine-based ligand (3,3′,5,5′-tetrakis(4-pyridyl)bimesityl) and a single metal ion.[18] The achiral zinc and cadmium frameworks formed possess lower porosity (44 and 46%, respectively) than **5**, due to the presence of several methyl groups in the 3,3′,5,5′-tetrakis(4-pyridyl)bimesityl ligand, which can protrude into the channels. The considerably greater porosity found in the TCPPDA-based framework **5** can be attributed to the lack of these methyl groups and the larger overall size of the ligand.

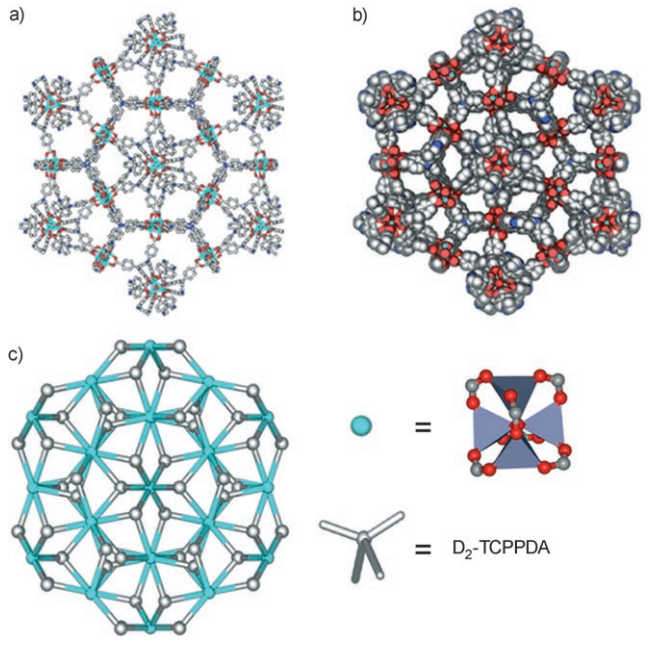

Figure 10. a) View of the network of **5** along [111]; b) space-filling model: in both (a) and (b), zinc atoms are indicated in aqua, nitrogen atoms in blue, carbon atoms in gray, and oxygen atoms in red; c) **5** is simplified as the corundum network by modeling the ligand as a tetrahedral connector (gray) and the octahedral SBU as a six-connected node (aqua).

Unlike frameworks **1** and **3**, all the D_2-TCPPDA ligands in **5** appear as either the $^{\delta}D_2$ or the $^{\lambda}D_2$ form, thus, the whole structure is enantiopure and homochiral; the crystals have the $I4_132$ space group. To the best of our knowledge, complex **5** represents the first chiral MOF possessing corundum topology. Preliminary second harmonic generation (SHG) measurements showed that **5** displays a response in the powder state that is three times greater than that of urea; this is a slightly stronger SHG response than that of some chiral MOFs constructed from chiral organic ligands.[17,19]

The results of thermogravimetric analysis (TGA) for complexes **3**–**5** measured under N_2 are shown in Figure 11. For

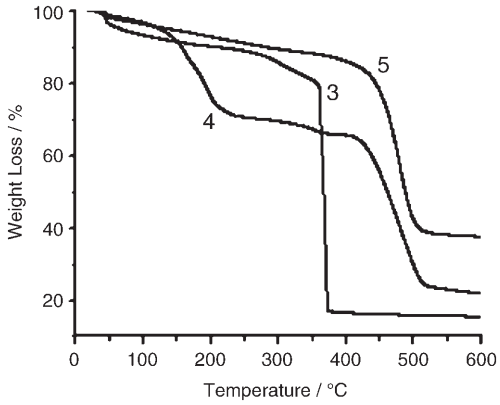

Figure 11. TGA plot of **3**, **4**, and **5**.

3, the weight loss of 27% from 50 to 350°C corresponds to the loss of four free DEF molecules and five free water molecules (calcd: 26.8%). For **4**, the weight loss of 30% from 50 to 245°C corresponds to the loss of three free DMSO molecules, five free water molecules, and three coordinated DMSO molecules (calcd: 32%). There is no further weight loss from 245 to 400°C. TGA shows that the framework of **5** is stable up to 410°C: from 50 to 300°C, there is a gradual weight loss of 7.7%, corresponding to the loss of one DMF and one water solvate trapped within the lattice (calcd: 7.3%), with no further weight loss from 300 to 410°C.

Gas sorption measurements for N_2 and H_2 were performed on compounds **1**, **2**, and **5**, and are shown in Figures 12 and 13, respectively. Complex **4** was unable to retain its framework after solvate removal. As-synthesized samples of **1** and **2** were exchanged with methanol to remove DMSO

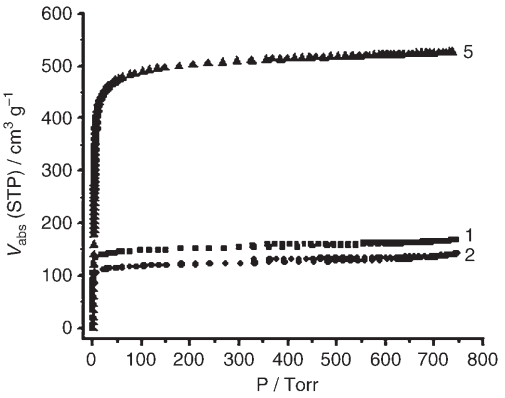

Figure 12. N_2 gas sorption isotherms of **1**, **2**, and **5** measured at 78 K.

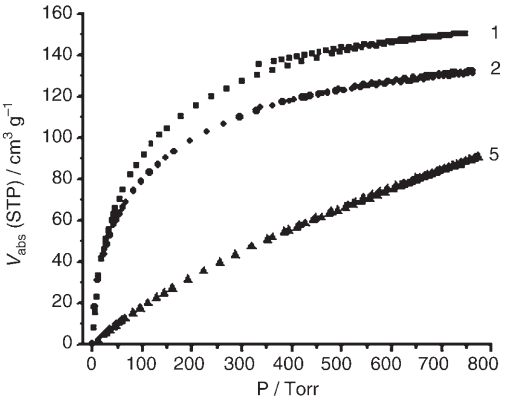

Figure 13. H_2 gas sorption isotherms of **1**, **2**, and **5** measured at 78 K.

and water molecules, then dried under vacuum overnight. N_2 sorption at 77 K (Figure 12) shows that complexes **1** and **2** possess Type I isotherms with Langmuir surface areas of 626 and 504 $m^2 g^{-1}$, respectively.[11] The hydrogen-storage capabilities of both compounds (14 $mg g^{-1}$ for **1**, 12 $mg g^{-1}$ for **2**) are comparable to reported values for "isoreticular" MOFs with high reported surface areas.[20] The difference in the nitrogen- and hydrogen-storage capacities of the two isomers is attributed to the variation in porosity, consistent with structures and calculated potential solvent-accessible volumes. An as-synthesized sample of **5** was exchanged with chloroform to remove DMF and water solvates, then dried under vacuum overnight. N_2 sorption at 77 K shows that **5** also has a Type I isotherm with a Langmuir surface area of 2095 $m^2 g^{-1}$, indicating that **5** possesses permanent porosity. Although **5** possesses much higher porosity than **1** and **2**, hydrogen sorption measurement showed that **5** has very low hydrogen-storage capability (8 $mg g^{-1}$). The higher hydrogen-storage capacity of **1** and **2** may be attributable to the existence of open metal sites in these networks after removal of axially coordinated water molecules in the paddlewheel SBUs; these open metal sites may have a high affinity for H_2 molecules, and are absent in **5**.[21] This result also indicates that the degree of porosity is not the sole factor in determining gas adsorptivity.[22] The design and synthesis of highly porous MOFs with open metal sites for hydrogen storage has, thus, become a target for future work.

Photoluminescence measurements for **4** and **5** at room temperature show that these MOFs exhibit strong luminescence at $\lambda_{max} = 425$ and 423 nm, respectively, upon excitation at 276 nm (Figure 14). The emissions of complexes **4** and **5**

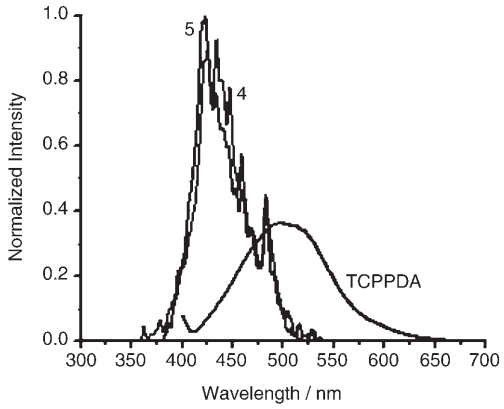

Figure 14. Emission spectra of **4** ($\lambda_{max} = 425$ nm), **5** ($\lambda_{max} = 423$ nm), and TCPPDA ligand ($\lambda_{max} = 498$ nm) in DMF solutions, upon excitation at 276 nm.

can be assigned to an intraligand $\pi^* \rightarrow \pi$ transition, because the free TCPPDA possesses similar emission ($\lambda_{max} = 498$ nm) in solution, although a sizable blue-shift (approx. 75 nm) is observed in the complexes. Photoluminescent emission by **4** and **5** is considerably more intense than that of the free ligand; this may be explained in terms of ligand rigidity. In solution at room temperature, TCPPDA exists in all three forms and is much more flexible than the forms within a MOF; this rigidity of the coordinated ligand effectively reduces the loss of energy, thereby increasing fluorescent efficiency.[23]

Conclusion

We have solvothermally synthesized five novel porous metal–organic frameworks based on a rationally designed tetracarboxylate ligand, TCPPDA, which exhibits stereoisomerism. This ligand can adopt two different geometries: pseudotetrahedral (D_2-TCPPDA) and rectangular (C_{2h}-TCPPDA). By varying the reaction temperature and/or metal species, porous frameworks containing either a single geometry (**1**, **2**, **3**, and **5**) or mixed geometries (**4**) of the ligand can be successfully isolated. Most interestingly, a chiral porous framework possessing the corundum topology can be constructed in a zinc complex (**5**), in which only $^{\delta}D_2$- or $^{\lambda}D_2$-TCPPDA are present in each crystal. These results demonstrate that a pseudorigid ligand that can adopt different geometries has significant advantages over a rigid one in the construction of coordination networks: such a ligand can adopt different geometries, according to the reaction conditions, to meet the coordination requirements of the metal

ion or metal-containing SBU. This provides a new strategy in the synthesis of MOFs with various structural topologies. In the future, the design and synthesis of additional organic ligands that have this advantageous mix of structural rigidity and conformational flexibility will be a powerful tool in the construction of MOFs with desirable topologies and functionalities.

Experimental Section

All starting materials were obtained commercially and were used without further purification. Thermal gravimetric analyses (TGA) were performed under N_2 by using a Perkin–Elmer TGA 7 analyzer. A Beckman Coulter SA 3100 surface-area analyzer was used to measure gas adsorption. Photoluminescence spectra were obtained by using a Perkin–Elmer LS 50B luminescence spectrometer. Solution NMR spectra were recorded by using a Bruker 200 MHz spectrometer. Elemental analyses (C, H, N) were performed by Canadian Microanalytical Services.

Synthesis of L1: (Scheme 1) 1,4-benzenediamine (0.5 g, 4.6 mmol), *tert*-butyl-4-bromobenzoate (5.0 g, 19 mmol), palladium acetate (45 mg, 0.20 mmol), tri-*tert*-butyl-phosphine (32 mg, 0.33 mmol), sodium *tert*-butoxide (2.3 g, 24 mmol), and toluene (20 mL) were mixed in an N_2 drybox. The reaction mixture was removed from the drybox and heated under N_2 at 75 °C for 24 h with constant stirring. The resulting brown mixture was poured into a saturated aqueous solution of ammonium chloride, and the aqueous layer was extracted with toluene. The combined organic phases were dried with anhydrous $MgSO_4$. Crude product was concentrated and purified by flash chromatography to give **L1** as a light yellow solid (1.8 g, 48 %). ^{1}H NMR (200 MHz, CD_3Cl): $\delta = 1.62$ (s, 36 H), 7.08 (s, 4 H), 7.12 (d, 8 H), 7.95 ppm (d, 8 H); ^{13}C NMR (200 MHz, CD_3Cl): $\delta = 28.66$, 81.22, 122.92, 126.69, 131.32, 150.88, 165.75 ppm.

Synthesis of H_4TCPPDA (*N,N,N′,N′*-tetrakis(4-carboxyphenyl)-1,4-phenylenediamine): **L1** (0.25 g) was dissolved in CH_2Cl_2 (20 mL), to which trifluoroacetic acid (0.5 mL) was added; the resulting yellow solution was allowed to stir at RT overnight. The yellow precipitate that formed was filtered, washed with CH_2Cl_2, and dried under vacuum to give H_4TCPPDA as a yellow solid (0.175 g, 96 %). ^{1}H NMR (200 MHz, CD_3Cl) $\delta = 7.08$ (s, 4 H), 7.12 (d, 8 H), 7.95 ppm (d, 8 H).

Synthesis of 3: A mixture of $[Co(en)_3]I_3 \cdot H_2O$ (15 mg, 0.024 mmol, en = ethylene diamine) and H_4TCPPDA (2.5 mg, 0.043 mmol) in *N,N*-diethylformamide (DEF) (1.5 mL) was sealed in a thick-walled glass tube under vacuum. The tube was heated at 120 °C for 5 d, then cooled to RT at a rate of 0.1 °C min^{-1}. The resulting red-violet crystals were washed with DEF to give **3**. Composition of **3** was determined by crystal structure analysis and TGA.

Synthesis of 4: A mixture of $Nd(NO_3)_3 \cdot 6H_2O$ (20 mg, 0.046 mmol) and H_4TCPPDA (2.5 mg, 0.043 mmol) in dimethylsulfoxide (DMSO) (1.0 mL) and pyridine (0.5 mL) was sealed in a thick-walled glass tube under vacuum. The tube was heated at 90 °C for 24 h, then cooled to RT at a rate of 0.1 °C min^{-1}. The resulting yellow rod crystals were washed with DMSO to give **4**. Elemental analysis calcd (%) for **4**: C 43.89, H 4.44, N 2.44; found: C 43.63, H 3.91, N 2.44.

Synthesis of 5: A mixture of $Zn(NO_3)_2 \cdot 6H_2O$ (20 mg, 0.067 mmol) and H_4TCPPDA (2.5 mg, 0.043 mmol) in *N,N*-dimethylformamide (DMF) (1.5 mL) was sealed in a thick-walled glass tube under vacuum. The tube was heated to 120 °C for 24 h and cooled to RT at a rate of 0.1 °C min^{-1}. The resulting red block crystals were washed with DMF to give **5** (2.5 mg, 71 %). Elemental analysis calcd (%) for **5**: C 52.08, H 3.16, N 4.50; found: C 51.49, H 3.15, N 4.79.

Crystal structure determination: Single-crystal X-ray diffraction was performed by using a Bruker Apex D8 CCD diffractometer equipped with a fine-focus sealed-tube X-ray source ($Mo_{K\alpha}$ radiation, $\lambda = 0.71073$ Å, graphite monochromated) operating at 45 kV and 40 mA. Crystals of **3**, **4**, and **5** were mounted on glass fibers and maintained under a stream of N_2 at 213 K. Frames were collected with 0.3° intervals in φ and ω for 30 s per frame, such that a hemisphere of data was collected. Raw data collection and cell refinement were achieved by using SMART; data reduction was performed by using SAINT+ and corrected for Lorentz and polarization effects.[24] Absorption corrections were applied by using the SADABS routine. Structures were solved by direct methods by using SHELXTL and were refined by full-matrix least-squares on F^2 by using SHELX-97.[25] Non-hydrogen atoms were refined with anisotropic displacement parameters during the final cycles. Hydrogen atoms were placed in calculated positions with isotropic displacement parameters set to $1.2 \times U_{eq}$ of the attached atom. The solvent molecules in **3**, **4**, and **5** are highly disordered, and attempts to locate and refine the solvent peaks were unsuccessful. Contributions from these solvent molecules to scattering were removed by using the SQUEEZE routine of PLATON; structures were then refined again by using the data generated.[15]

Compound **3**: $0.21 \times 0.20 \times 0.15$ mm, dark red-violet block, $C_{68}H_{42}Co_3N_2O_{16}$, $M_r = 1347.85$ g mol^{-1}, triclinic, $P\bar{1}$, $a = 13.703(3)$ $b = 14.120(3)$ $c = 15.810(4)$ Å, $\alpha = 105.069(4)$ $\beta = 103.355(4)$ $\gamma = 109.052(5)$°, $V = 2619.6(10)$ Å^3, $Z = 1$, $\rho_{calcd} = 0.854$ g cm^{-3}, $\mu = 0.513$ mm^{-1}, $F(000) = 687$, total reflections = 7120, independent reflections = 6303, $R_1 = 0.0515$, $wR_2 = 0.1325$, ($R_1 = 0.1059$, $wR_2 = 0.1707$ before SQUEEZE), GOF = 0.801, residuals based on $[I > 2\sigma(I)]$, $\Delta\rho_{max,min} = 0.279$, -0.468 e Å^{-3}.

Compound **4**: $0.2 \times 0.2 \times 0.2$ mm, light-yellow block, $C_{57}H_{48}N_3Nd_2O_{15}S_3$, $M_r = 1399.68$ g mol^{-1}, triclinic, $P\bar{1}$, $a = 15.156(3)$ $b = 15.657(2)$ $c = 26.967(4)$ Å, $\alpha = 81.603(16)$ $\beta = 78.042(12)$ $\gamma = 73.529(12)$°, $V = 5977.3(15)$ Å^3, $Z = 1$, $\rho_{calcd} = 0.389$ g cm^{-3}, $\rho = 0.472$ mm^{-1}, $F(000) = 699$, total reflections = 30569, independent reflections = 25476, $R_1 = 0.0819$, $wR_2 = 0.1837$, ($R_1 = 0.1762$, $wR_2 = 0.2249$ before SQUEEZE), GOF = 0.749, residuals based on $[I > 2\sigma(I)]$, $\Delta\rho_{max,min} = 2.533$, -2.866 e Å^{-3}.

Compound **5**: $0.48 \times 0.41 \times 0.60$ mm, red block, $C_{102}H_{60}N_6O_{26}Zn_8$, $M_r = 2308.71$ g mol^{-1}, cubic, $I4_132$, $a = b = c = 38.3364(9)$ Å, $\alpha = \beta = \gamma = 90$°, $V = 56342(2)$ Å^3, $Z = 8$, $\rho_{calcd} = 0.544$ g cm^{-3}, $\mu = 0.697$ mm^{-1}, $F(000) = 9296$, total reflections = 77336, independent reflections = 3273, $R_1 = 0.0374$, $wR_2 = 0.0624$, ($R_1 = 0.1399$, $wR_2 = 0.2763$ before SQUEEZE), GOF = 0.793, residuals based on $[I > 2\sigma(I)]$, $\Delta\rho_{max,min} = 0.075$, -0.145 e Å^{-3}, Flack parameter 0.09(2).

CCDC-287825, CCDC-287826, and CCDC-270804 contain the supplementary crystallographic data for this paper. These data can be obtained free of charge from the Cambridge Crystallographic Data Centre via www.ccdc.cam.ac.uk/data_request/cif.

Acknowledgements

This work was supported by the National Science Foundation (CHE-0449634), Miami University, and the donors of the American Chemical Society Petroleum Research Fund. H.C.Z. also acknowledges the Research Corporation for a Research Innovation Award and a Cottrell Scholar Award. The diffractometer was funded by NSF grant EAR-0003201.

[1] T. L. Hennigar, D. C. MacQuarrie, P. Losier, R. D. Rogers, M. J. Zaworotko, *Angew. Chem.* **1997**, *109*, 1044–1046; *Angew. Chem. Int. Ed. Engl.* **1997**, *36*, 972–973.

[2] a) P. J. Hagrman, D. Hagrman, J. Zubieta, *Angew. Chem.* **1999**, *111*, 2798–2848; *Angew. Chem. Int. Ed.* **1999**, *38*, 2639–2684; b) S. Kitagawa, R. Kitaura, S.-I. Noro, *Angew. Chem.* **2004**, *116*, 2388–2430; *Angew. Chem. Int. Ed.* **2004**, *43*, 2334–2375; c) E. Lee, J. Heo, K. Kim, *Angew. Chem.* **2000**, *112*, 2811–2813; *Angew. Chem. Int. Ed.* **2000**, *39*, 2699–2701; d) T. J. Prior, D. Bradshaw, S. J. Teat, M. J. Rosseinsky, *Chem. Commun.* **2003**, 500–501.

[3] a) L. Carlucci, G. Ciani, D. M. Proserpio, A. Sironi, *Angew. Chem.* **1995**, *107*, 2037–2040; *Angew. Chem. Int. Ed. Engl.* **1995**, *34*, 1895–1898; b) S. R. Batten, B. F. Hoskins, R. Robson, *J. Chem. Soc. Chem. Commun.* **1991**, 445–447; c) R. W. Gable, B. F. Hoskins, R. Robson, *J. Chem. Soc. Chem. Commun.* **1990**, 762–763; d) B. F.

Hoskins, R. Robson, N. V. Y. Scarlett, *Angew. Chem.* **1995**, *107*, 1317–1318; *Angew. Chem. Int. Ed. Engl.* **1995**, *34*, 1203–1204.
[4] D.-L. Long, A. J. Blake, N. R. Champness, C. Wilson, M. Schroder, *Chem. Eur. J.* **2002**, *8*, 2026–2033.
[5] L. R. MacGillivray, J. L. Reid, J. A. Ripmeester, *Chem. Commun.* **2001**, 1034–1035.
[6] H. Abourahma, B. Moulton, V. Kravtsov, M. J. Zaworotko, *J. Am. Chem. Soc.* **2002**, *124*, 9990–9991.
[7] a) A. J. Blake, N. R. Brooks, N. R. Champness, M. Crew, D. H. Gregory, P. Hubberstey, M. Schroder, A. Deveson, D. Fenske, L. R. Hanton, *Chem. Commun.* **2001**, 1432–1433; b) E.-Q. Gao, Z.-M. Wang, C.-S. Liao, C.-H. Yan, *New J. Chem.* **2002**, *26*, 1096–1098.
[8] a) W. Bi, R. Cao, D. Sun, D. Yuan, X. Li, Y. Wang, X. Li, M. Hong, *Chem. Commun.* **2004**, 2104–2105; b) Y. Kim, D.-Y. Jung, *Chem. Commun.* **2002**, 908–909.
[9] a) E.-Y. Choi, K. Park, C.-M. Yang, H. Kim, J.-H. Son, S. W. Lee, Y. H. Lee, D. Min, Y.-U. Kwon, *Chem. Eur. J.* **2004**, *10*, 5535–5540; b) S. R. Batten, *J. Solid State Chem.* **2005**, *178*, 2475–2479.
[10] a) I. S. Lee, D. M. Shin, Y. K. Chung, *Chem. Eur. J.* **2004**, *10*, 3158–3165; b) C.-Y. Su, A. M. Goforth, M. D. Smith, H.-C. zur Loye, *Inorg. Chem.* **2003**, *42*, 5685–5692; c) J.-P. Zhang, Y.-Y. Lin, X.-C. Huang, X.-M. Chen, *Chem. Commun.* **2005**, 1258–1260; d) N. Masciocchi, S. Bruni, E. Cariati, F. Cariati, S. Galli, A. Sironi, *Inorg. Chem.* **2001**, *40*, 5897–5905; e) I. Boldog, J. Sieler, K. V. Domasevitch, *Inorg. Chem. Commun.* **2003**, *6*, 769–772.
[11] D. Sun, Y. Ke, T. M. Mattox, B. A. Ooro, H.-C. Zhou, *Chem. Commun.* **2005**, 5447–5449.
[12] a) C. Janiak, *Dalton Trans.* **2003**, 2781–2804; b) C. N. R. Rao, S. Natarajan, R. Vaidhyanathan, *Angew. Chem.* **2004**, *116*, 1490–1521; *Angew. Chem. Int. Ed.* **2004**, *43*, 1466–1496; c) M. Eddaoudi, D. B. Moler, H. Li, B. Chen, T. M. Reineke, M. O'Keeffe, O. M. Yaghi, *Acc. Chem. Res.* **2001**, *34*, 319–330.
[13] a) J. C. Stephens, M. A. Khan, R. P. Houser, *Inorg. Chem.* **2001**, *40*, 5064–5065; b) M. Eddaoudi, J. Kim, M. O'Keeffe, O. M. Yaghi, *J. Am. Chem. Soc.* **2002**, *124*, 376–377.
[14] Y. Ke, D. J. Collins, D. Sun, H.-C. Zhou, *Inorg. Chem.* **2006**, ASAP ic051900p.
[15] A. L. Spek, *J. Appl. Crystallogr.* **2003**, *36*, 7–13.
[16] M. O'Keeffe, M. Eddaoudi, H. Li, T. Reineke, O. M. Yaghi, *J. Solid State Chem.* **2000**, *152*, 3–20.
[17] Z.-R. Qu, H. Zhao, Y.-P. Wang, X.-S. Wang, Q. Ye, Y.-H. Li, R.-G. Xiong, B. F. Abrahams, Z.-G. Liu, Z.-L. Xue, X.-Z. You, *Chem. Eur. J.* **2004**, *10*, 53–60.
[18] R. Natarajan, G. Savitha, P. Dominiak, K. Wozniak, J. N. Moorthy, *Angew. Chem.* **2005**, *117*, 2153–2157; *Angew. Chem. Int. Ed.* **2005**, *44*, 2115–2119.
[19] S. P. Anthony, T. P. Radhakrishnan, *Chem. Commun.* **2004**, 1058–1059.
[20] J. L. C. Rowsell, A. R. Millward, K. S. Park, O. M. Yaghi, *J. Am. Chem. Soc.* **2004**, *126*, 5666–5667.
[21] B. Chen, N. W. Ockwig, A. R. Millward, D. S. Contreras, O. M. Yaghi, *Angew. Chem.* **2005**, *117*, 4823–4827; *Angew. Chem. Int. Ed.* **2005**, *44*, 4745–4749.
[22] a) L. Pan, M. B. Sander, X. Huang, J. Li, M. Smith, E. Bittner, B. Bockrath, J. K. Johnson, *J. Am. Chem. Soc.* **2004**, *126*, 1308–1309; b) J. L. C. Rowsell, O. M. Yaghi, *Angew. Chem.* **2005**, *117*, 4748–4758; *Angew. Chem. Int. Ed.* **2005**, *44*, 4670–4679.
[23] L.-Z. Cai, W.-T. Chen, M.-S. Wang, G.-C. Guo, J.-S. Huang, *Inorg. Chem. Commun.* **2004**, *7*, 611–613.
[24] *SAINT+*, Bruker Analytical X-Ray Systems, Madison, WI, **2001**.
[25] G. M. Sheldrick, *SHELX-97*, Bruker Analytical X-Ray Systems, Madison, WI, **1997**.

Received: October 28, 2005
Published online: February 23, 2006

